Large magnetic fields and direct electric energy after P+B11 nuclear fusion measured at the Pulsotron-3 reactor

J. L. Lopez Segura[1], Arpan Pal[1], N. Urgoiti Moinot[1]

[1]*Advanced Ignition SL* C/francisco Medina Y Mendoza, Parcela 1, Poligono 19171 - (Cabanillas Del Campo) - Guadalajara*, Spain*

In this article, an efficiency of a group of Energy Recovery Coils (ERC), which were mounted in the Z-pinch type fusion device is described and the measured results of two tests T3073 and T3074 performed in 28 August, 2020 are presented in this paper. Tests were conducted by the Spanish Startup Advanced Ignition SL that operates the Z-pinch nuclear fusion reactor Pulsotron-3 loaded with Hydrogen-Boron (H+B11) thermonuclear fuel. The ERC were used to recover the electric energy directly from the plasma for the first time in the world and ERCs storing the energy in several large capacitors. During the test T3073 and T3074 the energy recovery capacitors recovered 22.59% and 17.74% of the injected energy at the target. Furthermore, a MAG-4 sensor measured the confinement time and the extremely large magnetic fields that were generated during the experiments. Experiments with the nuclear fuel generate magnetic field of more than 4 megateslas. Comparing to the experiments to the experiments with a dummy load (just hydrogen, but no boron), the peak magnetic field was 20-34 times larger and the stabilised magnetic field was 12-18 times larger. Thus, nuclear fusion generates large magnetic fields. In the proposed Pulsotron-3 technology thermonuclear fuel is utilised to generate clean electric power without CO_2 footprint and with reduced electricity cost. This industrial approach is a promising solution that can reduce world emissions to zero in less than 8 years.

jlopez@advancedignition.eu

I.   Introduction

The global energy consumption is predicted to grow by nearly 50% between 2020 and 2050 [1]. By 2050 the energy usage in industrial sector (refining, mining, manufacturing, agriculture, and construction) and transportation sector will increase by 30% and 40%, respectively. The rising income, urbanization and improved access to electricity will lead to ever growing demand for energy in residential and commercial sector and by 2050 energy consumption in these sectors will increase by 65%. Fulfilling this massive demand for energy in an environmentally responsible manner will be an extremely difficult challenge [2]. Currently, 80% of global energy is generated by burning the fossil fuels [3]. Due to this enormous demand the fossil reserves are rapidly depleting. Fossil fuel consumption still ramped up 2.9 % in 2018, driven by natural gas, which contributed 40% of this increase [16]. So these fossil fuels could run out in just over 50 years. The limited resources in the ground aren't even the biggest problem, there are plenty of downsides of burning fossil fuels that have severe effects on the climate and the environment. A portfolio approach is needed to decrease the dependence on fossil fuel and satisfy the energy demand. A possible solution is to improve the efficiency of energy usage by deploying strict regulation. However, it cannot provide the ever-growing primary energy generation that is needed to deliver a decent standard of living in the developing world, where 1.5 billion people still lack electricity. Therefore,

J. L. Lopez Segura et al.

J. Technol. Space Plasmas, **Vol.1**, Issue 1 (2021)

research and development of renewable energy is required before they are ready to be deployed on a large scale. Nuclear fusion [4]-[7] as renewable energy resource is a promising candidate for the long term. The nuclear fusion promises safe and ample clean electricity from the combination of small nuclei to release large amounts of energy with only non-toxic and short-lived nuclear waste as by-products [8].

This paper reports on two attempts at fusion energy recovery performed in the Pulsotron-3 and target charged with the use of diborane (B_2H_6) thermonuclear fuel. Pulsotron-3 is an inertial nuclear fusion reactor of the z-pinch type installed in an industrial facility located at Guadalajara, Spain. It is an upgraded version of the Pulsotron-2 that was the first one to be certified to reach fusion ignition conditions (Pulsotron-2 measured the ignition conditions using a dummy load but could not be loaded with thermonuclear fuel because has not radiation shields). The simple description of the Pulsotron-3 Z-pinch fusion: the device is loaded with a nuclear fuel through which a high current pulse is run. The current creates a magnetic field pulse. In the process a lot of heat and magnetic pressure is generated, thus the target turns into plasma. If more than a thousand megabars pressure is reached, nuclear fusion reactions are generated and high energy alpha particles are released in the process. After the current pulse passes, the compression is finished; the magnetic pressure becomes lower than the internal plasma pressure generated due to the heat and can no longer contain the plasma. Thus, the plasma explodes in a form of expanding plasma ball [17].

The Pulsotron-3 (see the schematics in Fig. 1.) is equipped with a capacitor bank that discharges the energy by using a switch throwing several megaamperes through the target loaded with nuclear fuel. Its power input is 40kW and the design output power is 400kW. The device is equipped with a sensor that can detect the movement of the plasma after the explosion of the target. Advanced Ignition installed also a group of Energy Recovery Coils (ERCs) adjacent to the target to recover electric energy directly from the plasma due nuclear fusions and plasma expansion. In addition, a magnetic sensor MAG-4 with three induction coils and 2 additional electric dipoles was used to measure the magnetic fields and plasma ball Time OF Flight (TOF) [9]-[10].

The nuclear fuel can be stored in gas form and compressed inside a cylinder at a controlled pressure and it can comprise of deuterium or boron hydride that can be injected there using diborane (B_2H_6) or obtained by evaporating decaborane ($B_{10}H_{14}$) or evaporating boron in an hydrogen atmosphere. In order to calibrate the sensors and check the reactor before the tests the reactor is filled with hydrogen as a dummy load similar to the nuclear fuel to be tested. Then a calibration shot is performed.

When the operation starts and the magnetic field is generated it propagates from the target to the magnetic sensors, where it is detected. And when the plasma ball starts to propagate, the electric field is measured with the two dipoles. The position of the coils and dipoles on the MAG-4 sensor can be seen in Fig. 2. The TOF measured using dipoles and magnetic sensors is similar but can be seen more accurately in the dipoles that measures less noise. The speed of the plasma can be obtained accurately as well with an accurate estimation of the plasma confinement time: If the distance from target to dipole-1 is d_1 and t_1 is the time from the electric current pulse switch-on until the plasma reaches the first dipole is t_1, and equivalently, d_2 and t_2 for the second dipole, then the plasma speed and the confinement time can be obtained by using the following formulas for the plasma speed v_p and the confinement time t_c:

$$v_p = \frac{d_2 - d_1}{t_2 - t_1} \qquad (1)$$

$$t_c = t_1 1 - \frac{d_1}{v_p} \qquad (2)$$

A confinement time larger than zero indicates that the plasma propagation has begun with a time-delay after the start of the current pulse. That means that the magnetic field is effective in compressing the plasma in the target and, thus, the plasma is confined. An optional third dipole takes into account the plasma acceleration.

In this experiment, two tests were performed T3073 and T3074; both were very similar but in the second one a high-density material (tin) was used to reflect ultraviolet light against the target. Test setup. Fig. 1 shows the test configuration consisting of Pulostron-3 and ERCs. C1 is the main capacitor bank that is initially charged at 89% of its maximum voltage (it was damaged due to an internal explosion which prevents the fusion reactor reaching maximum power). A transmission line (Tline) transmits the energy stored at C1 to the target by using a switch S1. A group energy recovery coils (ERCs) is installed adjacent to the target. Target and ERCs are coupled through the plasma which is placed

J. L. Lopez Segura et al.

J. Technol. Space Plasmas, **Vol.1**, Issue 1 (2021)

between them. The ERCs recover the electric energy directly from the plasma. The better is the coupling between the target and ERCs, more energy is recovered. The capacitor bank C2 is connected in parallel and stores the energy after the fusion. The stored energy at C2 is measured by measuring the voltage at capacitor leads by using voltage probes (Vprobe) as shown in the Fig. 1.
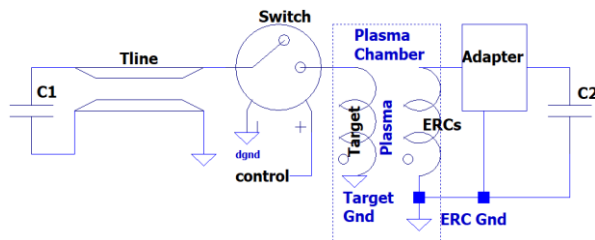

Figure 1: Test setup for tests T3073 and T3074: Pulsotron-3 and ERCs configuration. Plasma chamber fixes the target, compressing and ERC coils.

A group of magnetic sensors MAG-4 is installed on the Pulsotron-3 as much close as possible to the target and it measures the TOF and the magnetic field. Fig. 2 shows the configuration of the Mag-4 sensor. In [10], detail configuration and working principles are presented. Three inductor coil-1 (L1), coil-2 (L2) and coil-3 (L3) of the MAG-4 sensor measures the magnetic field [11]-[12]. The magnetic field at the target is measured by interpolating the magnetic field measured at the MAG-4 sensors and its distance to the target [13]-[15].
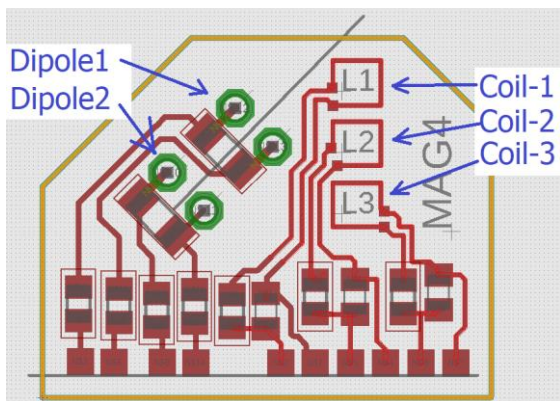

Figure 2: MAG-4 Magnetic sensors and dipoles.

As shown in Tab. 1 the Mag-4 magnetic sensor frequency response is very flat and ranges from 482.3 Hz to 4.5 GHz. However, the oscilloscope used in the test measures up to 4 GHz. Therefore, the measurements are performed only up to maximum frequency of 4 GHz.

Parameter	Frequency Value
Low pass frequency	482.3E+0 Hz
High pass frequency	4.5E+9 Hz
Center frequency	1.5E+6 Hz

Table 1: MAG-4 specifications.

Two dipoles are also installed in the MAG-4 sensor to measure the TOF after the discharge and the electrical conductivity of the plasma as shown in Fig. 3. The dipoles are placed close to coil-2 and coil-3. It was found that the time to reach coil-2 is the same as the plasma arrival time to dipole-1. On the other hand, the plasma arrival time to coil-3 and dipole-2 are similar. The time scale of the exploding plasma is calculated by using a linear interpolation of the distance from dipoles 1 and 2 from the discharge point.
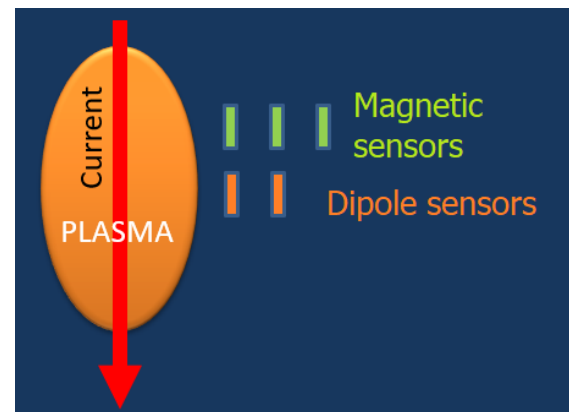

Figure 3: Magnetic sensors and dipoles measures TOF when plasma reaches them.

When the Pulsotron-3 main switch is triggered (Fig. 1), the stored energy in the capacitors (C1) discharges through the target to ionize and compress the thermonuclear fuel using an extreme magnetic field. The particles generated in the reactions due to nuclear fusion run out of the reactor and the energy was collected through the ERCs, which are magnetically coupled to the generated plasma. The collected energy is stored in the output capacitors C2 and can be used to power external loads.

II.   Test results

In this section, the results obtained from the test T3073 and T3074 are presented. The TOF can be measured by both MAG-4 sensor coils and dipoles. When the plasma generated by discharging current passes over the sensor coils, an almost digital change of the magnetic flux is

J. L. Lopez Segura et al.

J. Technol. Space Plasmas, **Vol.1**, Issue 1 (2021)

measured. Also, the dipoles detect that the plasma reaches them by changing the impedance and the voltage between both dipoles. When the plasma reaches the ERC coils, the recovered electrical energy is stored in the capacitor bank C2. It can be actively measured using the voltage probes across the capacitor leads.
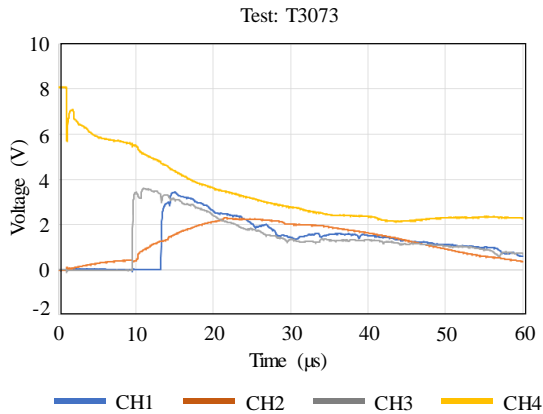

Figure 4: Measured TOF and recovered electric energy at test T3073 using dipoles. CH1: dipole 1, CH2: capacitor bank C2, CH3: dipole-2, CH4: capacitor bank C1.

Fig. 5 shows the TOF and recovered electrical energy for the test T3074. The TOF was measured to be 6.36 μs and 8.16 μs using dipole-1 and dipole-2, respectively. The TOF for the same events were measured also with the magnetic sensor coil-2 and coil-3. The values in this case were 6.45 μs and 8.21 μs, respectively. In the test T3074, 17.74% of the injected energy at the target was recovered at the capacitor bank C2, as shown in the Fig. 5.
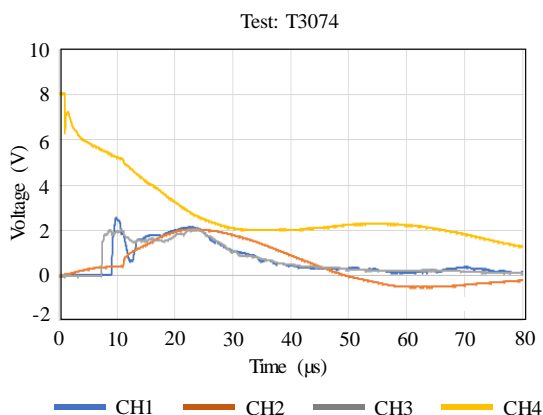

Figure 5: Measured TOF and recovered electric energy at test T3074 using dipoles. CH1: dipole 1, CH2: capacitor bank C2, CH3: dipole-2, CH4: capacitor bank C1. Figs. 4 & 5 show the TOF and recovered electrical energy for the test T3073 and T3074. Channels CH1 and CH3 correspond to the

voltage across dipole-2 and dipole-1, respectively. At channel CH2 the voltage at the electric energy recovery capacitor bank C2 was measured. CH4 corresponds to the voltage at main capacitor bank C1 of Pulsotron-3. The measurement of the TOF is useful because it can be used to know how much of energy was discharged in the target until it is damaged. This is done by obtaining the voltage of the capacitor bank C1 at the exact time the data from the TOF suggests that the plasma ball exploded. In Fig. 4 the test shot T3073 TOF was measured using dipole-1 and dipole-2 and it was 8.9 μs and 12.64 μs, respectively. Using the magnetic field sensors coil-2 and coil-3, the TOF was measured as 8.6 μs and 12.39 μs. The TOF can be measured from the sharp voltage drop in channel-4 that occurs in the main capacitor bank C1. As shown in the Fig. 4, it was found that the energy stored at test T3073 at the energy recovery capacitors (C2) was 22.59% of the injected energy at the target. The measured TOF and recovered electric energy are summarized in Tab. 2.

		T3073	T3074
TOF	Dipole-1	8.9 μs	6.36 μs
	Dipole-2	12.64 μs	8.16 μs
	Coil-2	8.6 μs	6.45 μs
	Coil-3	12.39 μs	8.21 μs
Recovered electric energy		22.59%	17.74%

Table 2: TOF measured at dipoles and coils and recovered electric energy at capacitor bank C2.

The magnetic field was measured using magnetic sensor coils of MAG-4. These new magnetic probes allow measuring an extremely high magnetic field up to frequencies of several GHz. When the target was unloaded (using a dummy load without fuel), the peak of measured magnetic field reached 550 kT. The magnetic field after stabilization was measured as 400 kT. In the test T3073 and T3074 the magnetic field was measured when the target is loaded with Hydrogen-Boron thermonuclear fuel. When Pulostron-3 was triggered a strong current of several millions of amperes went through the target. After the magnetic field vanished, a large detonation occurred when the generated plasma ball exploded. The magnetic probes in MAG-4 detected a very large magnetic field which was

measured using an oscilloscope. At channel-1 (CH1) of the oscilloscope the magnetic field at the coil-1 of the MAG-4 sensor was measured. It must be noted that the measured magnetic field is inverted due to the fact that the cable was installed in reverse direction. The magnetic field at coil-2 and coil-3 were measured at the channel-2 (CH2) and channel-3 (CH3), respectively. At channel-4 (CH4) the voltage of the Pulsotron-3 capacitor bank was measured. Figs. 6 and 7 shows the measured magnetic field and capacitor bank voltage at four channels of the oscilloscope for test T3073 and test T3074, respectively. In test T3073, a peak magnetic field of 17.3 megateslas was measured and a magnetic field of 7.36 MT is obtained after the stabilization. In test T3074, 10.3 MT of peak magnetic field of and 4.91 MT after the stabilization were measured. In following Figs. 6,7,8 and 9 the channels CH1,2 and 3 corresponds to the magnetic field obtained from magnetic sensors 1, 2 and 3 respectively. The CH4 is the measured voltage at the main capacitor bank C1.
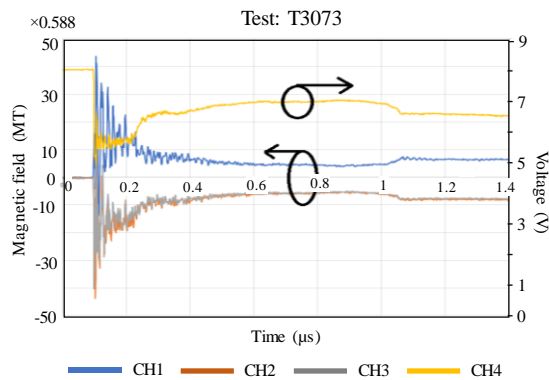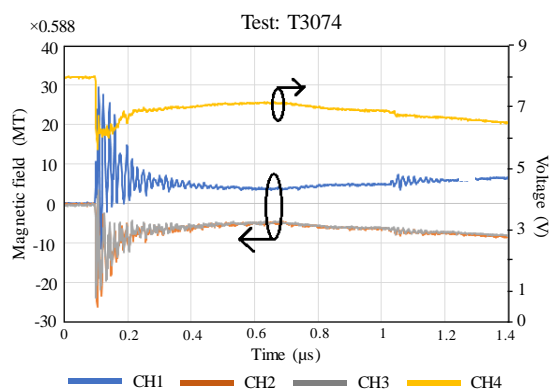
obtained from magnetic sensors 1, 2 and 3 respectively. The CH4 is the measured voltage at the main capacitor bank C1.

Further, Figs. 8 and 9 are similar to Figs. 6 and 7 obtained from the test T3073 and T3074, respectively. In Figs 8 and 9 the measured magnetic fields and capacitor bank voltage are presented for extended time to investigate the break time of the plasma ball. The channels in Figs 8 and 9 are the same as Figs. 6 and 7, respectively.

Tab. 3 summarizes the measured magnetic fields due to nuclear fusion in Pulsotron-3 during the test using unloaded target (dummy loads) and during tests T3073 and test T3074 when the target was loaded with hydrogen-Boron thermonuclear fuel.

Figure 6: Measured magnetic fields at test T3073. CH1, 2 and 3 corresponds to the magnetic field obtained from magnetic sensors 1, 2 and 3 respectively. The CH4 is the measured voltage at the main capacitor bank C1.

	Unloaded target (dummy loads)	The target loaded with thermonuclear fuel	
		T3073	T3074
Peak magnetic fields	550 kT	17.3 MT	10.3 MT
Stabilized magnetic fields	400 kT	7.36 MT	4.91 MT

Table 3: Measured peak and stabilized magnetic fields at test T3073 and T3074.

It was observed that during the tests with thermonuclear fuel the loaded target generated 20-34 times larger peak magnetic fields and 12-18 times larger stabilized magnetic fields comparee to the tests done using unloaded target (dummy loads).
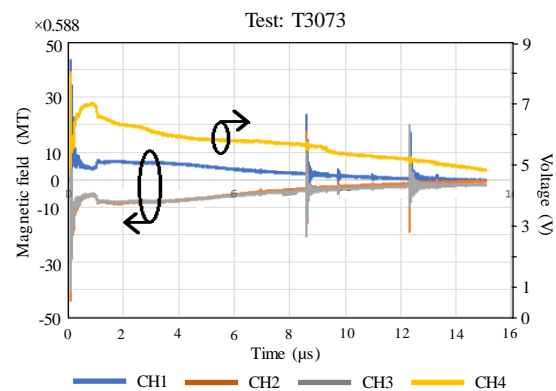

Figure 7: Measured magnetic fields at test T3074. CH1, 2 and 3 corresponds to the magnetic field

Figure 8: Measured magnetic fields at test T3073 for extended time period. CH1, 2 and 3 corresponds to the magnetic field obtained from magnetic sensors 1, 2 and 3 respectively. The CH4

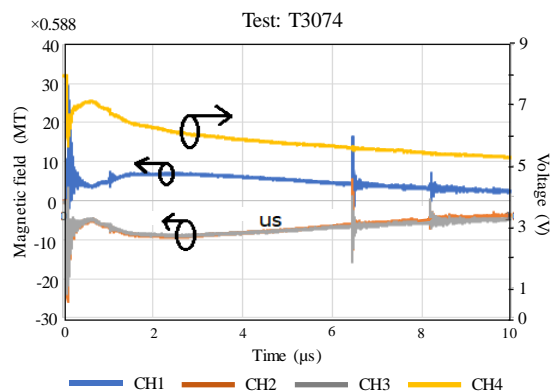is the measured voltage at the main capacitor bank C1.

Figure 9: Measured magnetic fields at test T3074 for extended time period. CH1, 2 and 3 corresponds to the magnetic field obtained from magnetic sensors 1, 2 and 3 respectively. The CH4 is the measured voltage at the main capacitor bank C1.

Differences between peak and stabilized magnetic fields: as can be seen in Figs. 6 and 7 the peak magnetic fields are AC peaks that appear during the first 200 nanoseconds of the discharge. The stabilized field appears after that and is a DC level that can last more than one microsecond.

III.   Conclusions

In this paper, the test results of two tests T3073 and T3074 are presented. These tests are performed using Pulsotron-3 which is Z-pinch type nuclear fusion reactor. For the test the target was charged with Hydrogen-Boron thermonuclear fuel. A group of ERCs recovered the electric energy directly from the plasma and stored in a large capacitor bank. The stored electric energy was measured at the capacitor leads using voltage probes. It was found that 22.59% and 17.74% of the injected energy at the target was recovered at the energy recovery capacitors during the test T3073 and T3074. These results prove the concept. However, Advanced Ignition intends to recover at least double the amount of energy that is injected into Pulsotron-3 in order to build energy generating reactors. To keep the energy in the recovery capacitor, diodes must prevent the discharge of the stored energy, but the charging current reaches amplitudes of megaamperes that could severely damage any existing commercial diode. Thus, in the future commercial reactor a set of diodes in parallel must be used, or another

method to avoid discharging is needed. It was simulated, that using several parallel SiC diodes 80% of the extracted energy can be stored.

A magnetic sensor MAG-4 was installed in adjacent to the target and used to measure the TOF of the plasma and the magnetic field generated due to nuclear fusion. Pulsotron-3 generated magnetic fields with amplitudes of more than 4 megateslas during these two tests. It is found that experiments with the target loaded with thermonuclear fuel generated 20-34 times larger peak magnetic fields and 12-18 times larger stabilized magnetic fields compared to the tests done using unloaded target (dummy loads). It is imperative that the large magnetic fields generated by nuclear fusions are measured and quantified with the high-speed magnetic probes like the ones used in this report, and added to QM in order to understand nuclear fusion and design new systems which will not only be able to ignite the fusion but also extract energy from it.

IV.   References

[1] IEA (2020), *World Energy Outlook 2020*, IEA, Paris,:   https://www.iea.Org/reports/world-energy-outlook-2020

[2] Intergovernmental Panel on Climate Change (IPCC) 2007 Climate change: synthesis report. World Meteorological Organization and United Nations. [Online] available: http://www.ipcc.Ch/publications_and_data/publications_ipcc_fourth_assessment_report_synthesis_report.htm

[3] D. Fasel and M. Tran, "Availability of lithium in the context of future D–T fusion reactors", Fusion Eng. Des. Vol. 75-79, pp. 1163–1168, Nov. 2005.

[4] T. F. R. Equipe, "Tokamak Plasma Diagnostics", Nucl. Fusion (1978), vol. 18, p. 647.

[5] H. Hutchinson, Principles of Plasma Diagnostics, 2nd ed.; Cambridge University Press: Cambridge, UK, 2002; Chapter 2.

[6] V. D. Pustovitov, "Magnetic Diagnostics: General Principles and the Problem of Reconstruction of Plasma Current and Pressure Profiles in Toroidal Systems," Nucl. Fusion (2001), vol. 41, p. 721.

[7] E. J. Strait, "Magnetic diagnostic system of the DIII-D tokamak". Nucl. Fusion 2006, vol. 77, no. 2, 2006.

J. L. Lopez Segura et al.

J. Technol. Space Plasmas, **Vol.1**, Issue 1 (2021)

[8] F. Romanelli, "Fusion Electricity: A roadmap to the realisation of fusion energy", Tech. rep., EDFDA (2012).

[9] N. Marconato, R. Cavazzana, P. Bettini, and A. Rigoni, "Accurate Magnetic Sensor System Integrated Design," *Sensors*, vol. 20, no. 10, p. 2929, May 2020.

[10] J. Segura, N. Urgoiti, and A. Pal, "AC Magnetic sensor to measure mega-amps current and kilo-tesla magnetic fields up to gigahertz frequencies," J. Technol. Space Plasmas, Vol. 1, no. 1,. 2020.

[11] L. C. Appel, M. J. Hole, "Calibration of the high-frequency magnetic fluctuation diagnostic in plasma devices," Rev. Sci. Instrum., Vol. 76, no. 9, 2005.

[12] S. Tumanski, "Induction coil sensors—A review," Meas. Sci. Technol., Vol. 18, no. 3, 19 Jan, 2007.

[13] J. C. Maxwell, "Treatise on Electricity and Magnetism", Oxford. Vol. 2, part. 4, ch. 2 (pp. 502-527) & ch. 23 (pp. 845-866), 1904.

[14] O. D. Jefimenko, "Electricity and Magnetism: An Introduction to the Theory of Electric and Magnetic Fields", Appleton-Century-Crofts (New-York - 1966). 2nd ed.: Electret Scientific (Star City - 1989), ISBN 978-0-917406-08-9.

[15] David J. Griffiths, Mark A. Heald, "Time-dependent generalizations of the Biot–Savart and Coulomb laws", American J Phys. 59 (2) (1991), 111-117.

[16] BP, Statistical Review of World Energy (2019) https://www.bp.com/content/dam/bp/business-sites/en/global/corporate/pdfs/energy-economics/statistical-review/bp-stats-review-2019-full-report.pdf

[17] U. Shumlak, "Z-pinch fusion", J. Appl. Phys., Vol. 127 (2020), p. 200901